Study on Finite Element Analysis of Breeze Vibration of Transmission Lines Based on Three-Node Cable Elements

Yi You[1], Longqin Zhang[1], Ling Zhang[1], Qinyong Ma[1], Zhitao Yan[2,*] and Xinpeng Liu[2]

[1]State Grid Xinjiang Electric Power Co., Ltd. Electric Power Research Institute, Urumqi, 830063, China
[2]School of Civil Engineering and Architecture, Chongqing University of Science and Technology, Shapingba District, Chongqing 401331, China

*Corresponding author e-mail: yanzhitao @cqu.edu.cn

Abstract. In order to study the mechanism of the breeze vibration of transmission lines, based on the non-linear model of Scanlan's experience, the finite element motion equation of the transmission line's breeze vibration is derived, and the dynamic solution is carried out. The results show that the parameters of Scanlan vortex force have a significant influence on the stable amplitude of the breeze vibration of transmission lines. Due to the neglect of the bending stiffness of the cable elements, the finite element calculation results of the cable breeze vibration are slightly less than the energy balance method, and as the wind speed increases, the error increases gradually; when the wind speed is 3m/s, the frequency of the wire vortex-induced vibration is 30Hz, which is consistent with the calculation of the Stokehal number.

1. Introduction

For the analysis and calculation of breeze vibration, the energy balance method [1] is widely used at home and abroad for decades. Due to the limited scope of application of the energy method and the large error, many researchers carried out the finite element analysis of the breeze vibration of the transmission line [2], and the breeze vibration load was obtained based on the input energy of wind energy. However, in practical engineering, focusing only on the steady-state response of the structure caused by vortex-induced vibration. Therefore, the simplified deterministic semi-empirical mathematical model has been widely used, especially the model of negative damping, such as Scanlan's [3-4] empirical nonlinear model has been widely used. In this paper, using the above model, the finite element equation of motion of the transmission line's breeze vibration is deduced, and the dynamic solution is solved by the time-history analysis. This analysis method can solve the problem of solving the dynamic equation of the breeze vibration, and can further consider the mass and boundary conditions of the hammer. Travel wave effects and bending stiffness of transmission lines.

2. Finite element model of breeze Vibration of transmission lines

In order to study the non-linear dynamic problem of the transmission line, the nonlinear dynamic equation of the cable must be established. To facilitate the establishment of mathematical models, the transmission line is simplified by the following basic assumptions: the bending stiffness, torsional

stiffness, and shear stiffness of transmission lines are ignored; large deformations and small strains of transmission lines are considered; parameters such as mass, tension, and elastic modulus does not change along the length of the transmission line.

2.1. Breeze Vibration Finite Element Equation

The breeze vibration of transmission lines is a typical geometric nonlinear problem. And its elongation deformation is generally considered to be a small linear elastic deformation range. Known by Hamilton principle:

$$\delta I = \delta \int_{t_1}^{t_2} \int_0^L (Q - V) ds dt + \int_{t_1}^{t_2} \int_0^L \delta W \, ds dt = 0 \tag{1.1}$$

Where: Q is the kinetic energy density; V A is elastic strain energy density; W A is the virtual power density.

$$Q = \frac{m}{2} \frac{\partial U^T}{\partial s} \frac{\partial U}{\partial s} \tag{1.2}$$

$$V = V_i + \frac{EA}{2} \varepsilon^2 + H(s)\varepsilon \tag{1.3}$$

$$\delta W = \partial U^T (F - c \frac{\partial U}{\partial s}) \tag{1.4}$$

$$\varepsilon = \varepsilon_0 + \varepsilon_l = \frac{dX^T}{ds} \frac{\partial U}{\partial s} + \frac{1}{2} \frac{\partial U^T}{\partial s} \frac{\partial U}{\partial s} \tag{1.5}$$

$$\boldsymbol{X} = \{x(s) \quad y(s) \quad z(s)\}^T \tag{1.6}$$

$$\boldsymbol{U} = \{u(s,t) \quad v(s,t) \quad w(s,t)\}^T \tag{1.7}$$

Where: m A is the unit length quality; c is the damping coefficient; F is the unit force; E is the elastic modulus; H is the tension of the cable; A A is the wire area; L is the length of the wire; x, y, z is the wire coordinates; u, v, w is the wire displacement.

Substituting (1.2) ~ (1.7) into (1.1), and then the Eq. (1.1) can be rewritten as:

$$\delta I = \delta \int_{t_1}^{t_2} \int_0^L \left[\frac{m}{2} \frac{\partial U^T}{\partial s} \frac{\partial U}{\partial s} - V_i - \frac{EA}{2} \left(\frac{dX^T}{ds} \frac{\partial U}{\partial s} + \frac{1}{2} \frac{\partial U^T}{\partial s} \frac{\partial U}{\partial s} \right)^2 - H \left(\frac{dX^T}{ds} \frac{\partial U}{\partial s} + \frac{1}{2} \frac{\partial U^T}{\partial s} \frac{\partial U}{\partial s} \right) ds dt \right] + \int_{t_1}^{t_2} \int_0^L \partial U^T (q + F - c \frac{\partial U}{\partial s}) ds dt = 0 \tag{1.8}$$

The three-node cable element is shown in Figure 1.1, and establish a local coordinate system:

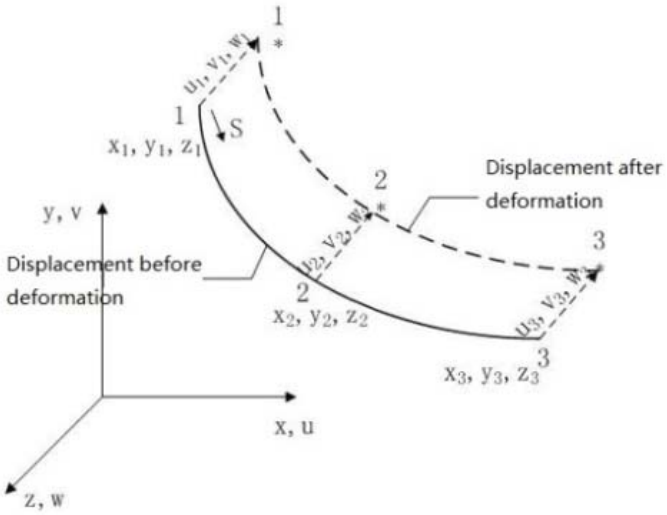

Figure 1.1. Cable element of three-node

The three-node cable element's shape function is:

$$N_1 = \frac{2s^2}{L_e^2} - \frac{3s}{L_e} + 1 \,, N_2 = -\frac{4s^2}{L_e^2} + \frac{4s}{L_e} \,, \; N_3 = \frac{2s^2}{L_e^2} - \frac{s}{L_e} \tag{1.9}$$

The shape function matrix is:

$$\boldsymbol{N} = \begin{bmatrix} N_1 \boldsymbol{I}_3 & N_2 \boldsymbol{I}_3 & N_3 \boldsymbol{I}_3 \end{bmatrix} \tag{1.10}$$

Therefore, the displacement vector of the node j is expressed as:

$$\mathbf{U}_j = \begin{Bmatrix} u_{1j} & v_{1j} & w_{1j} & u_{2j} & v_{2j} & w_{3j} & u_{3j} & v_{2j} & w_{3j} \end{Bmatrix}^T \tag{1.11}$$

According to equation (1.5), the relationship matrix of strain and displacement can be obtained:

$$\begin{cases} \boldsymbol{B}_0 = \begin{bmatrix} \boldsymbol{B}_{01} & \boldsymbol{B}_{02} & \boldsymbol{B}_{03} \end{bmatrix} \\ \boldsymbol{B}_l = \begin{bmatrix} \boldsymbol{B}_{l1} & \boldsymbol{B}_{l2} & \boldsymbol{B}_{l3} \end{bmatrix} \end{cases} \tag{1.12}$$

Substituting (1.11) ~ (1.12) into (1.8):

$$\mathbf{M}_j \ddot{\mathbf{U}}_j + \mathbf{C}_j \dot{\mathbf{U}}_j + \left(\mathbf{K}_{0j} + \mathbf{K}_{\sigma j} + \mathbf{K}_{1j} + \mathbf{K}_{2j} \right) \mathbf{U}_j = \mathbf{P}_j \tag{1.13}$$

In summary, the equations of motion are represented as global coordinates.

$$\boldsymbol{M}\ddot{\boldsymbol{u}} + \boldsymbol{C}\dot{\boldsymbol{u}} + \boldsymbol{K}\boldsymbol{u} = \boldsymbol{P} \tag{1.14}$$

Where: $\boldsymbol{M}$、 $\boldsymbol{K}$、 $\boldsymbol{C}$ is mass, stiffness and damping matrix respectively, $\boldsymbol{P}$ is the load vector.

2.2. Elemental stiffness matrix and element mass matrix

The element stiffness matrix is established in global coordinates and is expressed as follows:

$$\boldsymbol{K}_e = \boldsymbol{K}_{0e} + \boldsymbol{K}_{1e} + \boldsymbol{K}_{2e} + \boldsymbol{K}_{\sigma e} \tag{1.15}$$

Where $\boldsymbol{K}_{0e}$, $\boldsymbol{K}_{1e}$, $\boldsymbol{K}_{2e}$, $\boldsymbol{K}_{\sigma e}$ are linear stiffness, secondary nonlinear stiffness, cubic nonlinear stiffness, and geometric nonlinear stiffness matrix, respectively.

$$\boldsymbol{K}_{0e} = EA\int_0^L \boldsymbol{B}_0^T \boldsymbol{B}_0 ds \tag{1.16}$$

$$\boldsymbol{K}_{1e} = EA\int_0^L \left(\boldsymbol{B}_l^T \boldsymbol{B}_0 + 2\boldsymbol{B}_0^T \boldsymbol{B}_l\right) ds \tag{1.17}$$

$$\boldsymbol{K}_{2e} = 2EA\int_0^L \boldsymbol{B}_l^T \boldsymbol{B}_l ds \tag{1.18}$$

$$\boldsymbol{K}_{\sigma e} = \int_0^L H\boldsymbol{N}'^T \boldsymbol{N}' ds \tag{1.19}$$

The unit mass matrix is:

$$\boldsymbol{M}_e = m\int_0^{L_e} \boldsymbol{N}^T \boldsymbol{N} ds \tag{1.20}$$

2.3. Self-damping of Transmission Lines

This paper uses the self-damping theoretical expression derived by Lu M L [5].

$$P_c = 1.07\times10^6 E_{eq}\sqrt{k_D}k_s K_0 L\frac{D^{4.5} f^{6+\beta} A_0^{2.5}}{V_c^5} \tag{1.21}$$

Where: E_{eq} is the equivalent bending stiffness; k_D is an empirical factor, Steel core aluminum strand advisable 0.54, Steel wire advisable 0.65; A_0 is the maximum amplitude; k_s is the maximum bending stiffness reduction factor, advisable 0.5; for Steel core aluminum strand advisable $K_0 = 0.0042$, $\beta = -0.4256$. V_c is the wave speed of the transmission line, $V_c = L\sqrt{\frac{g}{8sag}}$; g is the gravitational acceleration, sag is the sag;

From the structural dynamics, the energy consumed by one cycle of the damping force is:

$$W = \int_0^{T_0} f\dot{y}dt = cA_0^2\omega^2\int_0^{T_0}\cos^2(\omega t-\varphi)dt = \pi C_c A_0^2\omega \tag{1.22}$$

Let the energy consumed by one cycle of a single degree of freedom system be equal to the energy consumed by one cycle of the self-damping transmission line, that is:

$$W = P_c T \tag{1.23}$$

Therefore, the equivalent self-damping C_c:

$$C_c = 1.07\times10^6 E_{eq}\sqrt{k_D}k_s K_0 L\frac{D^{4.5} f^{4+\beta} A_0^{0.5}}{2\pi^2 V_c^5} \tag{1.24}$$

With a classically damped n-degree-of-freedom system, the coordinate equation for each of the N breeze equations is:

$$M_n\ddot{q}_n + C_n\ddot{q}_n + K_n q_n = P_n \tag{1.25}$$

Where: $M_n = \phi_n^T m\phi_n$、$K_n = \phi_n^T k\phi_n$、$C_n = \phi_n^T c\phi_n$, M_n、C_n、K_n respectively are the n-th order generalized mass, generalized damping, generalized stiffness.

The damping ratio of the n- th mode shape is:

$$\zeta_n = \frac{C_n}{2M_n\omega_n} \tag{1.26}$$

According to the energy balance method, self-damping which is equivalent to wire self-damping theoretical expression simulates conventional viscous damping, is:

$$C_{cn} = C_n \tag{1.27}$$

Substituting the equation (1.26), the damping ratio of the n-th vibration mode is:

$$\zeta_n = \frac{C_{cn}}{2M_n\omega_n} = 1.07\times10^6 E_{eq}\sqrt{k_D}k_s K_0 L\frac{D^{4.5} f_n^{3+\beta} A_0^{0.5}}{8\pi^3 V_c^5} \tag{1.28}$$

2.4. Breeze vortex force

Based on Scanlan's empirical nonlinear model, the expression of wire vortex force is as follows:

$$F_y = \frac{1}{2}\rho U^2 D[Y_1(K)(1-\varepsilon\frac{v^2}{D^2})\frac{\dot{v}}{U} + Y_2(K)\frac{v}{D} + \frac{1}{2}C_L(K)\sin(\omega_{st}t+\phi)] \tag{1.29}$$

Studies show that $Y_2(K)$ and $C_L(K)$ can be ignored when locked, taking $Y_2 = Y_1\varepsilon$, so when the line reaches a stable amplitude, Equation (1.29) can be expressed as follows:

$$F_y = \frac{1}{2}\rho U^2 D\left(Y_1\frac{\dot{v}}{U} - Y_2\frac{v^2}{D^2}\frac{\dot{v}}{U}\right) \tag{1.30}$$

The load of the wire under the wind direction is:

$$F_z = \frac{1}{2}\rho U^2 D C_D \tag{1.31}$$

The load vector of the wire unit is:

$$\boldsymbol{F}_e = \int_0^L \boldsymbol{N}^T \begin{bmatrix} 0 & F_y & F_z \end{bmatrix} ds \tag{1.32}$$

3. Solving Dynamic Balance Equation

Solving the modal of (1.14), the mode shape vector can be obtained; then the transmission line vibration displacement can be expanded to:

$$\boldsymbol{u} = \boldsymbol{\Phi q} \tag{2.1}$$

Substituting (1.14):

$$\boldsymbol{I}\ddot{\boldsymbol{q}} + \tilde{\boldsymbol{K}}\boldsymbol{q} = \tilde{\boldsymbol{F}} - \tilde{\boldsymbol{C}}\dot{\boldsymbol{q}} \tag{2.2}$$

Where: $\tilde{\boldsymbol{K}}$ is generalized stiffness; $\boldsymbol{I}$ is a diagonal matrix; $\tilde{\boldsymbol{C}}$ is generalized damping, $\tilde{\boldsymbol{F}}$ is the generalized load.

$$\boldsymbol{I} = \boldsymbol{\Phi}^{\mathrm{T}}\boldsymbol{M}\boldsymbol{\Phi};\ \tilde{\boldsymbol{K}} = \boldsymbol{\Phi}^{\mathrm{T}}\boldsymbol{K}\boldsymbol{\Phi};\ \tilde{\boldsymbol{F}} = \boldsymbol{\Phi}^{\mathrm{T}}\boldsymbol{F}$$

Perform a dynamic time history analysis on equation (2.2), when $t = 0$: The initial displacement $\boldsymbol{q}_0$ and velocity $\dot{\boldsymbol{q}}_0$ are known, so at the first time step $t = \Delta t$, there is the following expression:

$$\boldsymbol{q}_{\Delta t} = \frac{\Delta t^2}{2}\left[\tilde{\boldsymbol{F}}_0 + \left(\frac{2}{\Delta t^2}\boldsymbol{I} - \tilde{\boldsymbol{K}}\right)\boldsymbol{q}_0 + \left(\frac{2}{\Delta t}\boldsymbol{I} - \tilde{\boldsymbol{C}}\right)\dot{\boldsymbol{q}}_0\right] \tag{2.3}$$

$$\dot{\boldsymbol{q}}_{\Delta t} = \frac{2}{\Delta t}\left(\boldsymbol{q}_{\Delta t} - \boldsymbol{q}_0\right) - \dot{\boldsymbol{q}}_0 \tag{2.4}$$

For subsequent time steps $t = 2\Delta t$, $3\Delta t$, …, $t + \Delta t$:

$$\boldsymbol{q}_{t+\Delta t} = \frac{\Delta t^2}{2}\left[\tilde{\boldsymbol{F}}_t + \left(\frac{2}{\Delta t^2}\boldsymbol{I} - \tilde{\boldsymbol{K}}\right)\boldsymbol{q}_t - \frac{1}{\Delta t^2}\boldsymbol{q}_{t-\Delta t} - \tilde{\boldsymbol{C}}\dot{\boldsymbol{q}}_t\right] \tag{2.5}$$

$$\dot{\boldsymbol{q}}_{t+\Delta t} = \frac{1}{2\Delta t}\left(3\boldsymbol{q}_{t+\Delta t} - 4\boldsymbol{q}_t + \boldsymbol{q}_{t-\Delta t}\right) \tag{2.6}$$

4. Analysis of examples

Taking the ground line of a certain section of the 1000KV transmission line project of the southeastern Shanxi ~ Nanyang ~ Jingmen as an example, the breeze vibration is analyzed. The span is 522m, the line type is JLB20B-240, the outer diameter is 0.02m, the unit length quality is 1.5955kg/m, and the average running tension is 40677.9N. The physical parameters of the wires are shown in Table 3.1. Computation procedures are programmed using MATLAB and calculated according to the above method.

Table 3.1. Physical parameters of single conductor

parameter name			unit	number
Sectional area	Aluminum (alloy)	A	mm^2	59.69
	Steel	A	mm^2	179.07
	The total area	A	mm^2	238.76
Comprehensive coefficient of elasticity		E	Pa	1.472×10^{11}
Calculate the total breaking force		T	N	3.152×10^{5}
Tension level component		H	N	4.068×10^{4}
Wire diameter		d	m	2×10^{-2}
The horizontal distance between two adjacent towers		L_x	m	522
Unit length quality		μ	$kg.m^{-1}$	1.5955

The transmission line damping is shown in Table 3.2:

Table 3.2. The damping ratio of the transmission line

Wind speed (m/s)	Vibration mode	Damping ratio (%)
2	261	0.010
2.5	306	0.024
3	363	0.036
3.5	408	0.049
4	449	0.070
4.5	486	0.097
5	523	0.13

Since the test object is a round and smooth steel bar that does not consider the surface roughness of the strand, there may be some differences. To accurately determine the vortex coefficient of the transmission line, it is necessary to retest the test contents of the above-mentioned documents.

Therefore, from Table 3.1 and Table 3.2, the coefficients used in this paper are shown in Figure 3.1 and Figure 3.2 respectively.

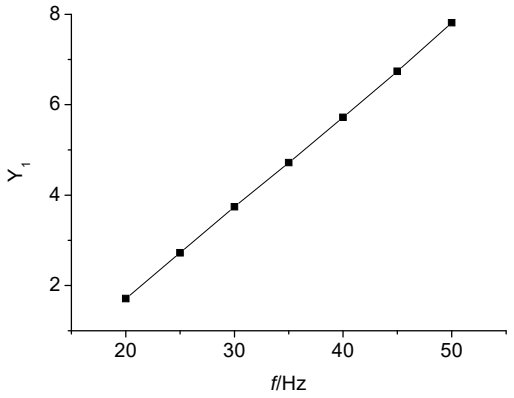

Figure 3.1. Value of Y1

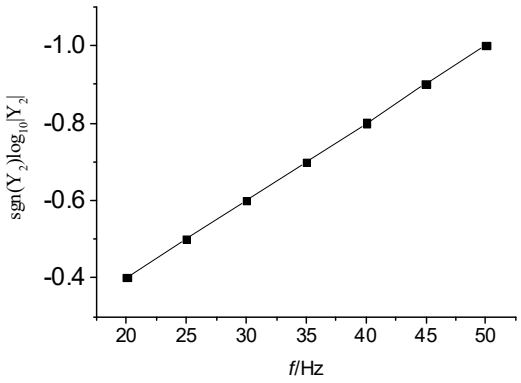

Figure 3.2. Value of Y2

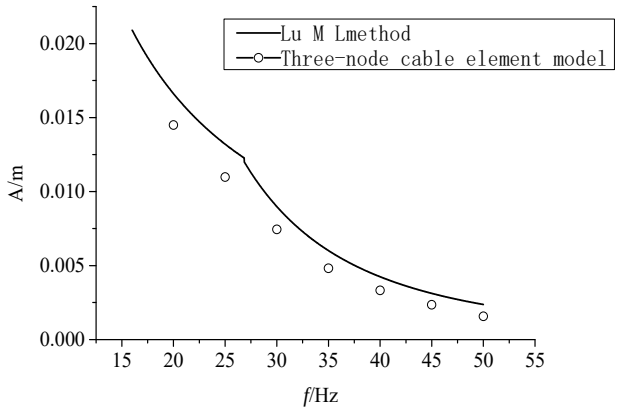

Figure 3.3. Comparison between three-node cable element model and Lu M L method

Take 7 typical wind speeds (2m/s~5m/s, interval 0.5m/s) for analysis, corresponding to the response frequency of the breeze vibration at 20Hz, 25Hz, 30Hz, 35Hz, 40Hz, 45Hz, and 50Hz. The result of the calculation are shown in Figure 3.3. As shown. When the wind speed is 2m/s~3m/s, the continuous curve in the figure is calculated according to the literature [6]. The calculation result is slightly smaller than that calculated by the energy balance method. With the increase of wind speed, the gap gradually increases. When the wind speed is 2m/s, the steady-state amplitude of the cable element model is 0.0145m, which is 12.65% less than that of the energy balance method. When the wind speed increases to 5m/s, the steady-state amplitude of the cable element model is 0.00157m, which is 33.76% less than that calculated by the energy balance method.

According to Fig.3.3, The gap between the calculation results through the three-node cable element model and the principle of energy balance has gradually increased. Since the energy balance method calculates the breeze vibration of the transmission line based on the experimental observation and induction of the wind input power and the self-damping power calculation formula of the transmission line, the influence of the bending stiffness of the transmission line is considered, However, the cable element model neglects the bending stiffness.When the cable element model is used to analyze the breeze vibration of the transmission line, due to the fact that the bending stiffness is not considered, with the increase of the locking frequency, the bending stiffness causes the self-damping of the transmission line that is greater than the bending stiffness when considering the bending stiffness. The increase gradually increases, leading to a gradual increase in the gap in results.

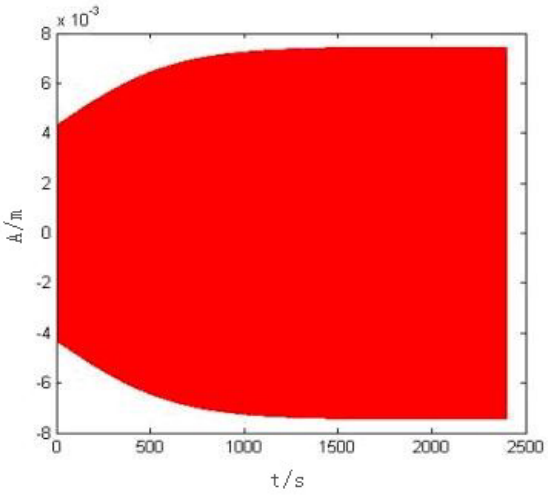

Figure 3.4. VIV of 3m/s wind velocity

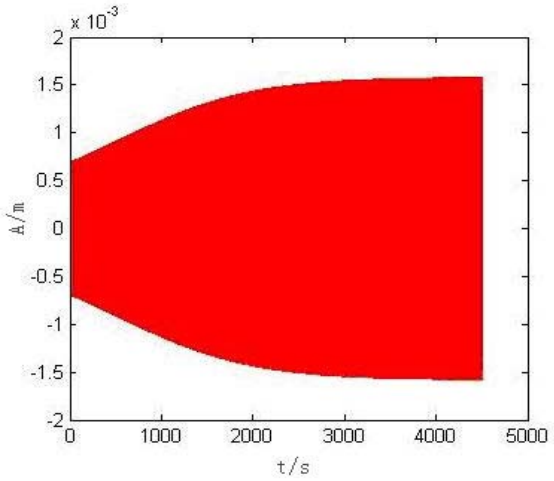

Figure 3.5. VIV of 5m/s wind velocity

Considering the space limitations, the time history curve of the breeze vibration at wind speeds of 3 and 5 m/s is selected here. And the calculation step length is taken as 0.001s. The calculation shows that the vibrations tend to be stable in the end.

5. Conclusion

(1) The change of the vortex force parameter of Scanlan determines the magnitude of the stable amplitude of the transmission line during the breeze vibration. With the increase of the wind speed, the vortex-induced vibration locking frequency of the transmission line increases, and the steady-state amplitude gradually decreases.

(2) The cable element model ignores the bending stiffness, and the cable element model is used to analyze the breeze vibration of the transmission line. Due to the fact that the bending stiffness is not taken into account, with the increase of the locking frequency, the bending stiffness causes the self-damping of the transmission line that is greater than the bending stiffness when considering the bending stiffness. The increase gradually increases, leading to a gradual increase in the gap in results.

(3) The steady-state response of the breeze-vibration resonance region calculated by the three-node cable element model is slightly smaller than that obtained by the energy method. With the increase of wind speed, the error gradually increases.

References

[1] Rawlins C B. The long span problem in the analysis of conductor vibration damping [J]. IEEE Transactions on Power Delivery. 2000, 15 (2): 770-776.

[2] Sauter D, Hagedorn P. On the hysteresis of wire cables in stockbridge dampers [J]. International Journal of Non-Linear Mechanics. 2002, 37 (8): 1453-1459.

[3] INDRANIL GOSWAMI, R H SCANLAN, N P JONES. Vortex-induced vibration of circular cylinders. I: experimental data [J] . Journal of Engineering Mechanics. 1993, 119 (11): 2271-2287.

[4] INDRANIL GOSWAMI , R H SCANLAN. N P JONES. Vortex-induced vibration of circular cylinders II :new model [J] . Journal of Engineering Mechanics. 1993, 119 (11): 2271-2287.

[5] Lu M L, Chan J K. An efficient algorithm for Aeolian vibration of single conductor with multiple dampers IEEE Transactions on power Delivery. 200722 (3): 1822-1529.